Rotation of Prismatic Rigid Porphyroblasts and Development of Internal Foliation: Results from Pixel-based Modelling Study

Youngdo Park

Dept. Earth and Environmental Sciences, Korea University, Sungbuk-ku Anam-dong 5-1, Seoul 136-701, Korea
Email: ydpark@mail.korea.ac.kr

Jin-Han Ree

Dept. Earth and Environmental Sciences, Korea University, Sungbuk-ku Anam-dong 5-1, Seoul 136-701, Korea

Won-Sun Jung

Dept. Earth and Environmental Sciences, Korea University, Sungbuk-ku Anam-dong 5-1, Seoul 136-701, Korea

Abstract: We have modelled rigid-body rotation of growing prismatic porphyroblasts and development of internal foliation formed by capturing external foliation. Jefferey equations (1922) were used for the porphyroblast rotation with the assumptions that porphyroblasts are mechanically rigid objects embedded in a deforming ductile matrix. The growth rule applied in this model is a simple expansion of crystal faces with known Miller indices with the pre-assigned growth rate for each face. The external foliation is assumed to have constant orientation. Parts of external foliation within the calculated volume of a porphyroblast are captured during the growth and rotated with the porphyroblast once they are captured.

During simple shear flow, prismatic porphyroblasts with every possible orientation with respect to the shear plane rotate constantly. The rate of rotation is determined as a function of strain rate and the shape and orientation of porphyroblasts. On the contrary, during pure shear flow, the longest axes of porphyroblasts approach toward the stretching direction. The observed patterns of the internal foliation within a porphyroblast are complicated in general, because the orientation of the rotation axis is not fixed with respect the kinematic reference frame. However, when there is pure shearing component in the flow geometry, porphyroblasts tend to have stable orientations and it is expected that Si patterns within a syntectonic porphyroblast can be straight. Thus, the straight Si patterns can be a good indicator for the flow geometry with some component of shear-direction-parallel stretching for syntectonic porphyroblasts. From the observations of model porphyroblasts, it is also proposed that central sections needs to be observed for the interpretation of internal foliations within prismatic porphyroblasts.

Table of Contents

Introduction

Internal foliations within porphyroblasts provide key information on relative timing of metamorphism with respect to regional deformation and relative rates of porphyroblast growth with respect to the rates of deformation [e.g., Zwart, 1962; Spry, 1963; Rosenfeld, 1970; Vernon, 1978, 1989; Bell and Johnson, 1989; Barker, 1994; Bell and Forde, 1995]. Much of these studies using the geometry of internal foliations has been carried out for garnet porphyroblasts [e.g. Rosenfeld, 1970; Gray and Busa, 1994; Jung et al., 1999] because internal foliations within garnets have relatively simple geometries. The basis of the simple geometries of internal foliations can be found in the rotation theory of Jeffery (1922) which predicts fixed rotation axis for spherical rigid objects with respect to the local kinematic reference frame (e.g. shear zone boundary). However, for porphyroblasts having non-spherical shape (e.g. andalusite and staurolite), there have been relatively few studies. This is because non-spherical or prismatic porphyroblasts do not have fixed rotation axis [Jeffery, 1922]. Therefore, the resulting patterns of internal foliations are complex [e.g. Jezek et al., 1999]. In this study, we present a computer model for simulating development of internal foliations in rotating prismatic porphyroblasts. It will also be shown how difficult or problematic it is to interpret internal foliations within prismatic porphyroblasts with the conventional two dimensional observation of thin sections.

Algorithms and Data Structure

Rotation of Porphyroblasts

For rotation of porphyroblasts, we have adopted the developed by Jeffery (1922). Details of the mathematical description can also be found in [Jezek et al, 1999]. Figure 1a illustrates the velocity field and velocity gradient tensor (V'_{ij}) with the external coordinate system (x'y'z'). Jeffery derived the sets of equations for rigid objects rotating in a viscous fluid matrix;

$$\omega_1 = B_1 E'_{32} - \Omega'_{32}$$
$$\omega_2 = B_2 E'_{13} - \Omega'_{13}$$
$$\omega_3 = B_3 E'_{21} - \Omega'_{21}$$

where w_i represents the angular velocities of an rigid objects around the internal axes (xyz, Figure 1b), and where:

$$E'_{ij} = \frac{1}{2}\left(V'_{ij} + V'_{ji}\right)$$

and:

$$\Omega'_{ij} = \frac{1}{2}\left(V'_{ij} - V'_{ji}\right)$$

The parameters B_1, B_2, and B_3 which are related to the shape of rigid objects, respectively, represents $(b^2-c^2)/(b^2+c^2)$, $(c^2-a^2)/(c^2+a^2)$, and $(a^2-b^2)/(a^2+b^2)$, and a, b, and c are axes of an ellipsoid object. Description for the orientation of rigid objects can be made much simpler by adopting Euler angles that relate internal coordinate system for rigid objects (xyz) and external coordinate system (x'y'z'). Freeman (1985) provided the solution for the rotation of rigid objects with Euler angles;

```
df/dt = (w₁·sin y + w₂·cos y) / sin q
dq/dt = w₁·cos y - w₂·sin y
dy/dt = w₃ - cos q
```

and f, q and y represents the Euler angles defined in Figure 1b and the quantities divided by dt represent the rate of changes in three Euler angles.

Figure 1. Velocity gradient tensor and coordinate systems
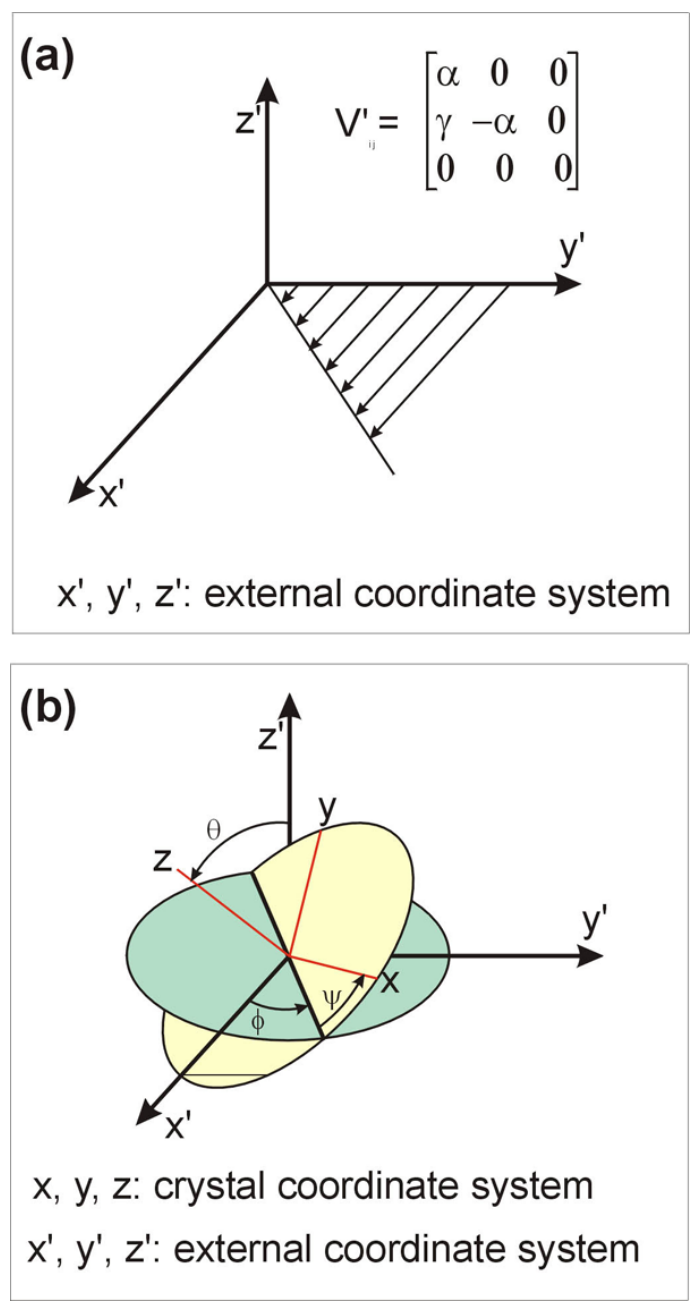
Velocity gradient tensor and coordinate systems.

a. Three dimensional velocity gradient tensor (V'_{ij}) for plane strain deformation in the rectangular coordinate system, x'y'z'.
b. Euler angles between external (x'y'z') and internal (xyz) reference frames.

Growth of Porphyroblasts

In two dimensions, an area occupied by a crystal with orthorhombic symmetry (a crystal with two sets of mutually perpendicular faces) can be represented with two sets of two parallel lines (Figure 2). If we let ($h_1 k_1 0$) to represent the Miller index of a face, the region between the two parallel faces can be described as,

$$h_1 \cdot x + k_1 \cdot y + 0 \cdot z < |A|$$

where A is a parameter related to the distance between the face and the origin. Similarly, for another face with the Miller index of ($h_2 k_2 0$), the region between these two faces is,

$$h_2 \cdot x + k_2 \cdot y + 0 \cdot z < |B|$$

where B is also a parameter similar to A. If a point satisfies the above two inequalities simultaneously, then the point is within the region surrounded by four faces. If we assign larger values for A and B (e.g. new A = old A + growth amount), the region surrounded by the four faces can expand, thus the crystal grows.

For three dimensions, we need three inequalities to define a volume occupied by a crystal with the faces of the Miller indices ($h_1 k_1 l_1$), ($h_2 k_2 l_2$), and ($h_3 k_3 l_3$).

$$h_1 \cdot x + k_1 \cdot y + l_1 \cdot z < |A|$$
$$h_2 \cdot x + k_2 \cdot y + l_2 \cdot z < |B|$$
$$h_3 \cdot x + k_3 \cdot y + l_3 \cdot z < |C|$$

where A, B, and C are parameters related to the distance between the face and the origin. A rectangular-box-shaped porphyroblast can grow by assigning larger values for A, B and C. The shape of the porphyroblast can be determined by relative magnitudes of A, B, and C.

http://virtualexplorer.com.au/

Figure 2. Definition of a crystal surrounded by two sets
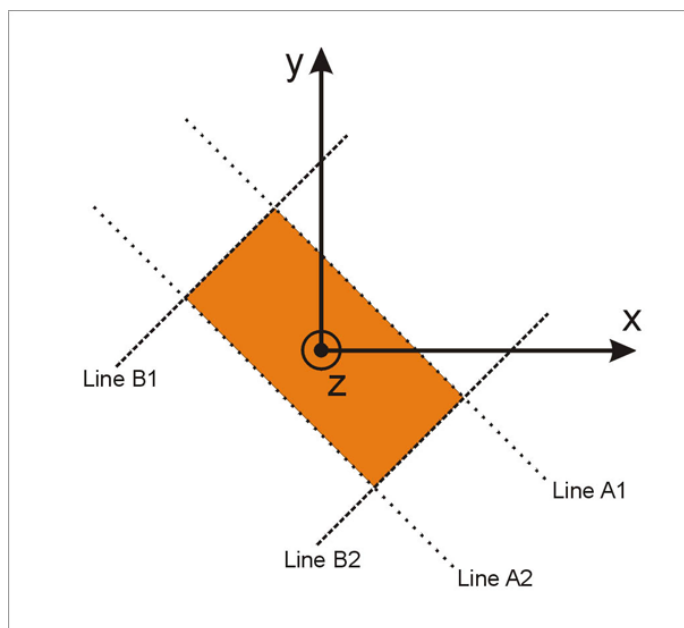
Definition of a crystal surrounded by two sets (A_1A_2A and B_1AB_2A) of parallel lines. See text for detail.

Data Structure, Algorithm, and Assumptions

The data structure for the model (Figure 2) is based on pixels (or volumetric pixels). The pixels within the model system have their coordinate information (x'y'z') and additional material information. The material information for each pixel can be among the following four types;

1. porphyroblast,
2. internal foliation within porphyroblast,
3. matrix,
4. external foliation within matrix (or future inclusions when they are entrapped).

Development of internal foliation patterns is performed by repeated growth and rotation (Figure 3). During growth, parameters of A, B, and C (described in the earlier section) becomes larger in each step of growth. Depending on the material information, the program replaces matrix with porphyroblast or external foliation with internal foliation as the crystal faces expand. To apply rotation for a porphyroblast, either porphyroblast or matrix can rotate. Here, we have adopted matrix rotation because it is much simpler but still gives the same internal fabric. If pixels have material information of porphyroblast or internal foliation, they remain stationary. On the other hand, pixels

occupied by external foliation rotate backward with the amount calculated using Euler angles.

One of the key assumptions made in this study is no dragging of external foliation by the rotation of a porphyroblast. This assumption is physically unrealistic, but we made this assumption because this makes algorithm much simpler and still produces complicated enough textures that may give some insights when interpreting natural textures. Therefore, the results made in this study would be simpler compared with the results made by studies that consider dragging of external foliation [Jezek et al., 1999]. However, these studies also have limitations because of the assumption of Newtonian rheology of the matrix. For successful modelling of natural rocks, a model has to be fully mechanical in order to model non-linear viscous flow in the matrix.

Figure 3. Algorithm for the development of internal foliations
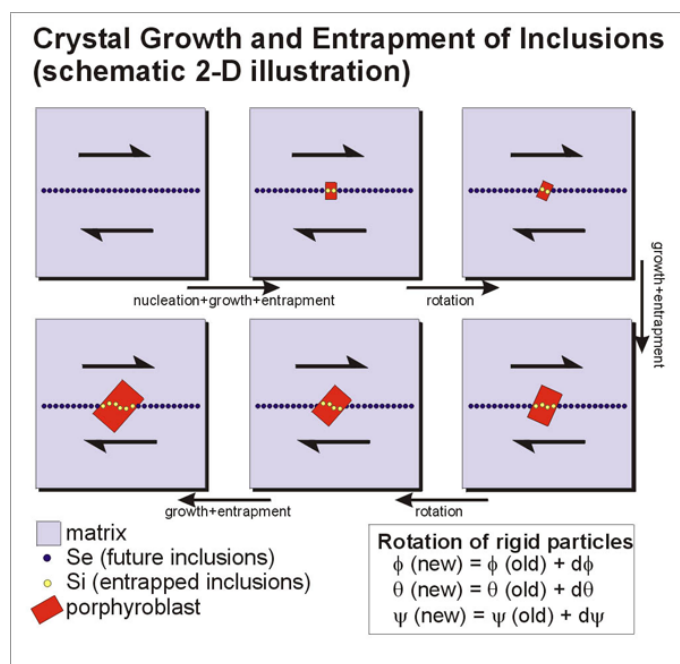
Algorithm for the development of internal foliations.

Results

A series of experimental runs were carried out to test the validity of results and to study the geometry of the internal foliations. Selected results for the axial ratio values of 1:1:3 (=shortest:intermediate:longest axis) for simple and pure shearing flow will be described here.

Figure 4 shows the trajectories of the crystal axes on stereograms. For simple shear flow (Figure 4a, b & c), it is shown that no stable orientation of porphyroblast exists. When one of the porphyroblast axis is set parallel to the y' axis (external axis) as the initial condition (Figure 4a & c), the initially y' axis-parallel porphyroblast axis remains stationary. The internal foliation for these cases will be familiar ones with the spiral type [e.g. Figure 7.33; Figure 7.37, Passchier and Trouw, 1996]. However, when none of the axes of a porphyroblast are aligned parallel to y' axis (Figure 4b), the porphyroblast keeps rotating while changing its rotation axis. The internal foliation pattern will be more complicated (discussed later). The trajectory of the longest axis (blue in Figure 4b) shows an elliptical pattern, known as Jeffery orbit [Freeman, 1985]. For pure shear flow (Figure 4d, e & f), the longest axis of a porphyroblast approaches to the shear direction. The rotation axis is also changing for these cases (Figure 4d, e & f), but it is expected that the rotation axis will be fixed when the longest axis is parallel to the y' direction. In general, when the porphyroblast axes are inclined to y' axis (or any of the external axes), the rotation axis keep changing its orientation regardless of the geometry of flow until the longest axis become parallel to y' axis for pure shear.

Figure 4. Stereographic projection
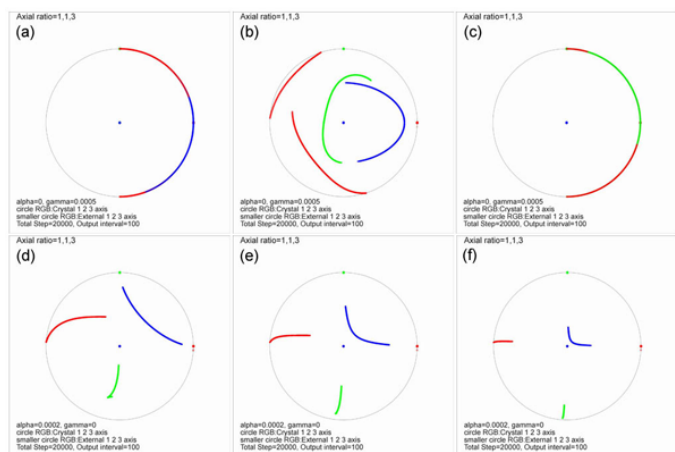
Stereographic projection of the trajectories of rotating crystal axes (axial ratio=1:1:3) at different starting orientations (top row: simple shearing flow, bottom row: pure shearing flow). Details of rotation history for each streogram can be seen in Figure 7. Blue:longest axis (axial lenght=3), Red & Green: shorter axes (axial length=1). Arrows indicate the initial orientation.

When the rotation and growth of algorithm are combined, three dimestional images consisting of volumetric pixels can be constructed (Figure 5 and 6). Figure 5 (a, b & c) shows serial sections cut normal to the external axes (x', y' and z'). The perfect monoclinic symmetry reflecting the monoclinic flow geometry is visible only on the central sections. Details of each experiment, including rotation histories and three dimensional perspective views, can be seen in Figure 7 .

Figure 5. Serial sections of a model porphyroblast

black: matrix, gray: porphyroblast, white: internal foliation (inclusions) or external foliation
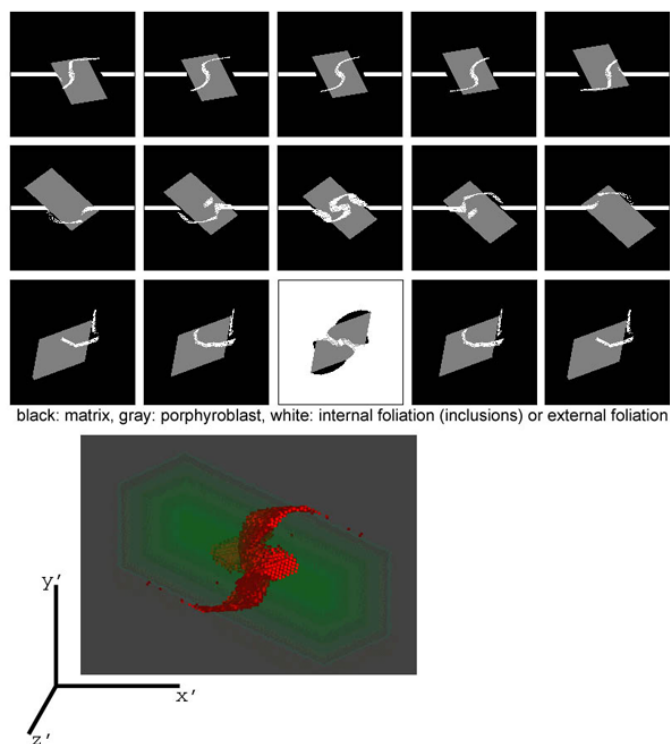
Serial sections of a model porphyroblast with rotation history of Figure 4b (top row: serial sections along the z axis, middle row: serial sections along the x axis, bottom row: serial sections along the y axis).

Figure 6. Perspective views of model porphyroblasts
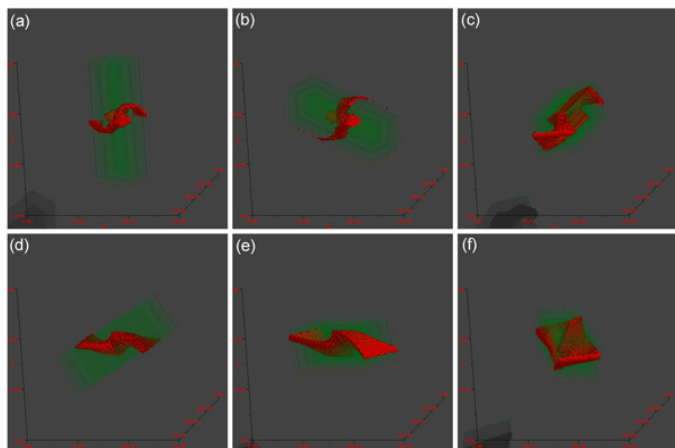
Perspective views of model porphyroblasts with rotation histories in Figure 4 (green: porphyroblast, red: internal foliation). (a) to (f) respectively correspond to Figure 4 (a) to (f).

Figure 1. Animations for crystal rotation and three dimensional view of the inclusion patterns

Animations for crystal rotation and three dimensional view of the inclusion patterns

Animations for crystal rotation and three dimensional view of the inclusion patterns. Figures (a) to (f) respectively correspond to Figure 4 (a) to (f).

a. rotation history, rotation history (movie) and 3-D view.
b. rotation history, rotation history (movie) and 3-D view.
c. rotation history, rotation history (movie) and 3-D view.
d. rotation history, rotation history (movie) and 3-D view.
e. rotation history, rotation history (movie) and 3-D view.
f. rotation history, rotation history (movie) and 3-D view.

Discussion and Conclusions

One of the major limitations of our model is that no dragging of external foliation occurs. Since dragging of external foliation (before being incorporated into internal foliation) by porphyroblast-matrix interaction does not occur in our model, the resulting geometry of the internal foliation will be simpler than the natural conditions where dragging occurs. Therefore, it is difficult to apply the model results for the interpretation of natural microstructures. Models that incorporates dragging effects [e.g. Jezek et al,

1999] will be more suitable for natural rocks, but these models will also have limitations because matrix rheology is assumed to be Newtonian. A multiple process model such as Elle [Jessell 2001] that allows crystal growth and local displacement calculations by fully mechanical codes may be the only solution for this type of modelling.

Although the model results can not be directly compared with the natural rocks, we feel that the model results may have some implications when interpreting the pattern of internal foliation within porphyroblasts. As demonstrated on the serial sections (Figure 5), the perfect monoclinic geometries are observed only on the central sections of a porphyroblast. Some of the sections lacking the monoclinic symmetry (Figure 5) can be misinterpreted. For example, they can be misinterpreted to develop when the porphyroblast post-tectonically captures a fold hinge that developed prior to porphyroblast growth. Therefore, it is suggested to observe microstructures on the central sections when interpreting kinematics from natural rocks.

During pure shear flow or general shear flow, prismatic porphyroblasts with larger axial ratio may have stable orientations (Figure 4). In this case, the syntectonic porphyroblasts can have straight internal foliations that are usually interpreted to be pre- or post-tectonic. Thus, it is suggested to be cautious when interpreting straight internal foliations within prismatic porphyroblasts. The question of syntectoic vs pre- or post-tectonic timing relation can be answered by combined examination of the distribution of the longest axis of porphyroblasts as well as the patterns of internal foliations. For example, straight internal foliations within porphyroblasts of a certain longest-axis orientation group and curved internal foliation within other orientation groups can be interpreted to synteconic growth at stable orientation with the flow geometry of general shear or pure shear.

In conlusion, our model, in spite of major limitations, produced results that can be helpful for microstructural examination of porphyroblasts. Two general statements for petrographic analyses of internal foliation can be made.

1. For the correct observation of internal foliations, observation plane should contain the central section of porphyroblast. Otherwise, the patterns of internal foliations may contain misleading microstructures for interpretation.
2. Straight inclusions within prismatic porphyroblasts do not always represent pre- or post-tectonic growth.

These microstructures need to be interpreted with caution because syntectonic straight inclusions can be formed at stable orientations when flow geometry is general or pure shear.

Acknowledgements

References

Barker, A. J., 1994. Interpretation of porphyroblast inclusion trails: limitation imposed by growth kinetics and strain rates. J. Metamorph. Geol., 12: 681-694.

Bell, T. H. and Forde, A., 1995. On the significance of foliation patterns preserved around folds by mineral overgrowth. Tectonophysics, 246: 171-181.

Bell, T. H. and Johnson, S. E., 1989. Porphyroblast inclusion trails: the key to orogenesis. J. Metamorph. Geol., 7: 279-310.

Freeman, B., 1985, The motion of rigid ellipsoidal particles in slow flows. Tectonophysics, 113, 163-183

Gray. N.H. and Busa, M.D., 1994, The three-dimensional geometry of simulated porphyroblast inclusion trails: inert-marker, viscous-flow models. J. Metamorph. Geol., 12, 575-587

Jeffery, G.B., The motion of ellipsoidal particles immersed in a viscous fluid. Proc. Royal Soc. Lond., 102, 161-179

Jessell, M. W., Bons P. D., Evans L., Barr T. D. & Stuwe K. 2001. Elle : the numerical simulation of metamorphic and deformation microstructures. Computers and Geosciences 27, 17-30.

Jezek, J., Saic, S., Segeth, K. and Schulmann, K., 1999, Three-dimensional hydrodynamic modelling of viscous flow around a rotating ellipsoidal inclusion. Computer s and Geoscience, 25, 547-558

Jung, W.S., Ree, J.-H. and Park, Y., 1999 Non-rotation of garnet porphyroblasts determined from 3-D inclusion trail data using serial polishing and reflected microscopy: an example from the Imjingang belt, South Korea. Tectonophysics, 307, 381-395

Rosenfeld, J. L., 1970. Rotated garnets in metamorphic rocks. Geol. Soc. Am., Spec. Pap., 129: 102pp.

Spry, A., 1963. The origin and significance of snowball structure in garnet. J. Petrol., 4: 211-222.

Vernon, R. H., 1978. Porphyroblast-matrix microstructural relationships in deformed metamorphic rocks. Geol. Rundsch., 67: 288-305.

Vernon, R. H., 1989. Porphyroblast-matrix microstructural relationships: recent approaches and problems. In: Daly, J. S., Cliff, R. A. and Yardley, B. W. D. (Eds.), Evolution of Metamorphic Belts. Geol. Soc. London, Spec. Publ., 43: 83-102.

Passchier, C. W., and Trouw, R. A. J., 1996. Microtectonics. Springer, Berlin, 289pp.

Zwart, H. J., 1962. On the determination of polymetamorphic mineral associations, and its application to the Bosost area (central Pyrenees). Geol. Rundsch., 52: 38-65.